Abnormal dorsal attention network activation in memory impairment after traumatic brain injury

Running title: *Network dysfunction and memory in TBI*

Emma-Jane Mallas[1], MSc, Sara De Simoni,[1] PhD, Gregory Scott[1], MRCP, PhD, Amy E. Jolly[1], MSc, Adam Hampshire[1,2], PhD, Lucia M. Li[1,2], MRCP, PhD, Niall J. Bourke[1], MSc, Stuart A.G. Roberts[1,3], MRCS, Nikos Gorgoraptis[1], MRCP, PhD, David J. Sharp[1,2,4], MRCP, PhD

[1]Computational, Cognitive and Clinical Neuroimaging Laboratory, Department of Brain Sciences, Imperial College London, London, UK.
[2] UK Dementia Research Institute, Care Research and Technology Centre, Imperial College London, London, UK
[3] Academic Department of Military Surgery and Trauma (ADMST), Royal Centre for Defence Medicine (RCDM), Birmingham, UK
[4]Royal British Legion Centre for Blast Injury Studies, Department of Bioengineering, Imperial College London, London, UK

Corresponding author: Prof. David Sharp

Computational, Cognitive and Clinical Neuroimaging Laboratory (C3NL), 3rd Floor Burlington Danes Building, Imperial College London, Hammersmith Hospital Campus, Du Cane Road, London, W12 0NN

david.sharp@imperial.ac.uk

Abstract

Memory impairment is a common, disabling effect of traumatic brain injury. In healthy individuals, successful memory encoding is associated with activation of the dorsal attention network as well as suppression of the default mode network. Here, in traumatic brain injury patients we examined whether: i) impairments in memory encoding are associated with abnormal brain activation in these networks; ii) whether changes in this brain activity predict subsequent memory retrieval; and iii) whether abnormal white matter integrity underpinning functional networks is associated with impaired subsequent memory. 35 patients with moderate-severe traumatic brain injury aged 23-65 years (74% males) in the post-acute/chronic phase after injury and 16 healthy controls underwent functional MRI during performance of an abstract image memory encoding task. Diffusion tensor imaging was used to assess structural abnormalities across patient groups compared to 28 age-matched healthy controls. Successful memory encoding across all participants was associated with activation of the dorsal attention network, the ventral visual stream and medial temporal lobes. Decreased activation was seen in the default mode network. Patients with preserved episodic memory demonstrated increased activation in areas of the dorsal attention network. Patients with impaired memory showed increased left anterior prefrontal activity. White matter microstructure underpinning connectivity between core nodes of the encoding networks was significantly reduced in patients with memory impairment. Our results show for the first time that patients with impaired episodic memory show abnormal activation of key nodes within the dorsal attention network and regions regulating default mode network activity during encoding. Successful encoding was associated with an opposite direction of signal change between patients with and without memory impairment, suggesting that memory encoding mechanisms could be fundamentally altered in this population. We demonstrate a clear relationship between functional networks activated during encoding and underlying abnormalities within the structural connectome in patients with memory impairment. We suggest that encoding failures in this group are likely due to failed control of goal-directed attentional resources.

Introduction

Memory impairments are among the most common and disabling consequences of traumatic brain injury (TBI) (Vakil, 2005) and are associated with poor functional outcome (Gillis and Hampstead, 2015). Episodic memory, the ability to remember discrete events, is impaired following TBI (Ricker *et al.*, 2001; Himanen *et al.*, 2006; Wright *et al.*, 2010). The degree of impairment varies substantially within this population (Chiou *et al.*, 2016; Vakil *et al.*, 2019).

Associative memory function after TBI is related to the structure and function of the medial temporal lobe (MTL) and its connections to other limbic structures (De Simoni *et al.*, 2016). Functional networks underlying memory processes rely on structural connections provided by white matter microstructure that are vulnerable to traumatic damage. TBI patients show widespread damage to structural connections (Wallace *et al.*, 2018), and disrupted communication between brain networks involved in memory function (Sharp *et al.*, 2011; Bonnelle *et al.*, 2012; Jilka *et al.*, 2014). The structure of key white matter tracts such as the fornix correlates with associative learning and memory in TBI patients and controls (Kinnunen *et al.*, 2011) and differences in white matter microstructure have been associated with heterogeneity of episodic memory in TBI (Chiou *et al.*, 2016).

Function of the memory system can be investigated using the subsequent memory (SM) paradigm. The neural basis for encoding impairments can be assessed by comparing functional activation during events later remembered versus forgotten. Over 100 studies have utilised this method in healthy adults (Uncapher and Wagner, 2009; Kim, 2011). Meta-analyses using the SM paradigm have identified activation of regions in the dorsal attention network (DAN), including inferior frontal junction, medial intraparietal sulcus (IPS), middle temporal area and inferior temporal cortex to indicate successful encoding (Kim, 2011, 2015). Conversely, activation of the default mode network (DMN) and regions including superior-frontal cortex, frontal pole, temporo-parietal junction, posterior cingulate cortex/precuneus, and anterior cingulate cortex/ventromedial prefrontal cortex predict subsequently forgotten items (Daselaar *et al.*, 2009; Kim, 2011; De Chastelaine *et al.*, 2015).

Episodic memory failures in TBI have been attributed to impaired attentional control (Vakil, 2005), which is partially supported by the functional imaging literature in this population. A small number of studies have investigated memory network function after TBI using the SM paradigm and reported hyperactivation compared to controls in lateral temporal lobes, left MTL, left parietal lobe (Gillis and Hampstead, 2015), frontoparietal network (Arenth *et al.*, 2012) and subcortical regions (Russell *et al.*, 2011), though others found no differences (Strangman *et al.*, 2008). These findings have been interpreted as compensatory activation drawing on other cognitive systems that support memory function (Russell *et al.*, 2011). However, in the absence of behavioural differences between patients and controls (Russell *et al.*, 2011; Arenth *et al.*, 2012) it is difficult to interpret the relationship of these effects with mnemonic deficits.

Previous work has not stratified TBI patients by impairment, nor considered structural and functional effects together. Here, for the first time, we investigate memory network function in TBI patients with and without episodic memory impairment, providing a more detailed understanding of the neural basis underlying post-traumatic episodic memory deficits. Using a SM paradigm with fMRI we examine activation patterns during long-term memory encoding. We use DTI to investigate differences in white matter integrity of individual tracts and structural connectomes of those with and without SM impairment. We specifically test the following hypotheses: i) TBI patients with impaired SM show altered functional activation during encoding compared to TBI patients with normal SM; ii) these changes will be apparent within the DAN and DMN iii) DTI measures of white matter integrity will be associated with SM impairment.

Subjects and Methods

Patient group and clinical details

48 TBI patients were recruited into the study. Thirteen were excluded following motion analysis (see 'Motion'). Therefore 35 patients were included in the imaging analysis (9 females, mean age=43.20±11.20; range=23-65 years). All patients were in the post-acute/chronic phase after injury (mean months since injury=126.78±158.88, range=3–436 months). Injuries were secondary to road traffic accidents (54%), falls (23%), military blast (11%), assault (6%) and sports injuries (6%). Patients were recruited from specialist TBI clinics and military rehabilitation units. All patients had moderate-severe injuries according to the Mayo classification system (Malec *et al.*, 2007). Exclusion criteria were: premorbid psychiatric or neurological illness; previous brain injury; drug or alcohol abuse; pregnancy or breastfeeding; or contraindication to MRI. The study was approved by the Hammersmith and Queen Charlotte's and Chelsea Research Ethics Committee, and the Ministry of Defence Research Ethics Committee (MODREC). All participants gave written informed consent in accordance with the Declaration of Helsinki.

Control group

16 healthy controls (6 females, mean age=38.19±11.99 years) were included in the SM imaging analysis. An independent control group (n=28) were used for the DTI analysis (9 females, mean age=37.01±5.32 years). Controls were recruited through the National Institute for Health Research (NIHR) Imperial Clinical Research Facility, London, UK and family members of patients. Exclusion criteria for controls were the same as for patients.

Neuropsychological assessment

A detailed neuropsychological battery was used to assess cognitive function in all participants. Immediate and delayed verbal recall were assessed using The Logical Memory I and II subtests of the Wechsler Memory Scale, third edition (WMS-III) (Wechsler, 1997). The People Test from the Doors and People Test battery was used to measure associative learning and recall (immediate and delayed) (Baddeley *et al.*, 1994). Premorbid intelligence was measured using the Wechsler Test of Adult Reading

(WTAR) (Wechsler, 2001). Nonverbal reasoning ability was assessed using the Matrix Reasoning subtest of the Wechsler Abbreviated Scale of Adult Intelligence (WASI).(Corporation, 1999) Inhibition and set-shifting were assessed using colour-word Stroop tests from the Delis-Kaplan Executive Function System (Delis *et al.*, 2001) and the Trail Making Test (forms A and B) were used to further assess executive functions (Reitan, 1958).

Subsequent memory task

Participants viewed a series of abstract art images while in the scanner, which they were asked to commit to memory and told they would be later tested on (Figure 1 'Encoding'). Images were presented for four seconds in blocks of six, with a fixation of one second between each image and 20 seconds between each block. A total of nine blocks consisting of 54 different images in total (6 unique images per block) were shown. No images were repeated. No response was required from participants during the scan. The fMRI scan was followed by further structural acquisition lasting for 15 minutes after which SM for the abstract art images was tested immediately upon exit from the scanner. Participants were shown 108 images (54 previously seen, 54 novel) and asked to indicate using a keyboard press (yes/no) whether they previously saw the image (Figure 1 'Retrieval'). Accuracy was determined using the sensitivity index (d'), a measure taken from signal detection theory which represents the probabilities of responses being a 'true hit' rather than a 'false positive'. A higher score represents greater discrimination between previously seen (remembered) and novel items during the post-scanner recognition test, thus accounting for potential response bias.

< Figure 1 >

Statistical analysis of demographic and behavioural data

Group characteristics (age and years of education), performance on neuropsychological assessments and accuracy on the SM paradigm were compared using one-way analysis of variance (ANOVA), with post-hoc independent samples t-tests (Welch's two-sample t-test) to assess which pairwise comparisons were driving significant main effects. All statistical analysis was performed in RStudio (v1.1.453). Age at injury and time since

injury were compared using independent samples t-tests. Chi-squared test was used to compare distribution of gender across the groups.

MRI acquisition

MRI data were obtained using a Philips Intera 3.0-T MRI scanner using Nova Dual gradients, a phased-array head coil, and sensitivity encoding with an undersampling factor of two. fMRI images were obtained using a T2*-weighted gradient-echo echoplanar imaging sequence (EPI) with whole-brain coverage (repetition time/echo time, 2000/30ms; 31 ascending slices with thickness 3.25mm, gap 0.75mm, voxel size 2.5x2.5x5mm, flip angle 90°, FOV 280x220x123mm, matrix 112x87). Quadratic shim gradients were used to correct for magnetic field inhomogeneities within the brain. T1-weighted whole-brain structural images were obtained in all subjects. The experimental paradigm was programmed using Matlab Psychophysics toolbox and stimuli were presented through an IFIS-SA system.

Diffusion-weighted volumes with gradients applied in 64 non-collinear directions were collected using the following parameters: 73 contiguous slices, slice thickness=2mm, FOV 224mm, matrix 128x128 (voxel size=1.75x1.75x2mm^3), b value=1000, and four images with no diffusion weighting (b=0s/mm^2).

Statistical analysis of imaging

Functional imaging analysis

Functional imaging analysis was performed using fMRI Expert Analysis Tool (FEAT), in FSL (Smith *et al.*, 2004). Image preprocessing involved realignment of EPI images, spatial smoothing using a 6mm full-width at half-maximum Gaussian kernel and temporal high-pass filtering using a cut-off frequency of 1/50 Hz. EPI functional datasets were registered into standard-space using individual high-resolution T1 images with FMRIB's Linear Image Registration Tool (FLIRT) (Jenkinson *et al.*, 2002). Cerebrospinal fluid and white matter signal was extracted using FMRIB's Automated Segmentation Tool (FAST) (Zhang *et al.*, 2001) and regressed out of the data in order to remove any artefactual noise from these sources. fMRI data were analysed using voxelwise time-series analysis within the framework of the general linear model. A design matrix was generated with a synthetic haemodynamic response function and its

first temporal derivative to account for the time lag between stimuli presentation and the measured response. To investigate the effect of SM impairments, brain activation was compared between successful and unsuccessful encoding trials at the subject-level by subtracting forgotten trials from remembered trials. The resulting lower-level contrast images were entered into independent samples t-tests at the higher-level. These between-groups contrasts were modelled with the demeaned age of each subject as a covariate. Clusters of contiguous voxels were defined using the default threshold of $z > 2.3$ in FSL, and resulting clusters were tested for significance using a cluster extent significance threshold of $p<0.05$. A 5mm sphere was constructed around the peak of the largest significant cluster of the higher-level effects and percentage in BOLD signal change was extracted from the voxels within these spheres.

Motion issues were dealt with in two ways. 1) Framewise displacement (FD), a measure of how much the head position changes from one frame to the next (Power *et al.*, 2012) was obtained for each volume using the FSL motion outliers tool. fMRI scans were excluded if movement exceeded 3mm for any volume or if >15% of volumes exceeded an FD of 0.5 (De Simoni *et al.*, 2018) 2) pre-processed fMRI data were subjected to ICA decomposition, and motion related components were removed using ICA-AROMA (Pruim *et al.*, 2015) by a semi-automated method. All components were visually inspected using spatial maps, time series, and power spectra, and those considered to be noise as per published guidance (Griffanti *et al.*, 2017) were removed.

Diffusion analysis

Diffusion data were corrected for motion artefacts and eddy currents, and brain-extracted using the brain-extraction tool (BET) (Smith, 2002) part of the FSL image processing toolbox (Smith *et al.*, 2004). A tensor model was then fitted to the data using FMRIB's Diffusion Toolbox (FDT) and, using FDT, we generated voxel-wise fractional anisotropy (FA) map. These maps were transformed into standard 1mm space using tensor based registration in DTI-TK (Zhang *et al.*, 2006) and tract-based spatial statistics (TBSS) (Smith *et al.*, 2006). Non-parametric permutation testing (n=10,000) with a threshold of $p<0.05$ was applied with age as a nuisance regressor to compare the skeletonised white matter between groups. FA values were extracted for each subject (i) within individual tracts as defined by the JHU White Matter Tracts atlas(Mori and Crain, 2005) as well as (ii) the cingulum from NatBrainLab (Catani and Thiebaut De

Schotten, 2008) and (iii) the mean across the whole white matter skeleton. DTI data for patients were compared to an independent group of healthy controls matched for age at the group level. The effect of group, tract and their interaction on FA was tested using a two-way ANOVA. One-way t-tests with false-discovery rate (FDR) multiple comparison corrections were used to compare between groups across tracts.

Structural connectome underpinning the memory networks

In order to better understand the relationship between the functional and structural imaging results, we targeted the white matter that specifically related to the task derived functional networks to create a structural connectome of the underlying white matter architecture. White matter networks were constructed to represent the structural connectivity underlying the functional networks produced by the task. Using the IIT Human Brain Atlas (Zhang and Arfanakis, 2018) FA was extracted for each of the track density (TDI) maps. These have been defined using tractography between all possible pairs of grey matter labels in the Desikan atlas (Desikan *et al.*, 2006), thus providing a white matter atlas of connectivity between cortical and subcortical regions of the brain. A 90x90 connectivity matrix of FA between each of the grey matter nodes was produced for each subject. Functional network activation maps, derived from the Correct-Incorrect contrast for regions of increased and decreased activation during successful encoding (Figure 3A) were binarized at a 50% probability threshold and the two resulting network masks were separately intersected with the Desikan grey matter parcellation to reveal the nodes of each network. FA values between each of the nodes were extracted from the structural connectivity matrices to inform the degree of connectivity between each node. Mean FA underlying each network was extracted and compared across groups. The influence of age on the mean connectivity values for each network was assessed by comparing linear models with and without age as an interaction term which was found to be non-significant for both encoding activation and encoding deactivation networks. Network connectivity was compared between groups on a node-by-node basis using the network-based statistic in NBS v1.2 (Zalesky *et al.*, 2010) implemented in MATLAB to perform 10,000 random permutations at a threshold of 3.1

Lesion Segmentation

Brain areas with focal lesions were masked using semi-automatic segmentation methods based upon an algorithm for geodesic image segmentation as described in (Criminisi *et al.*, 2008) and implemented in IMSEG v1.8. FLAIR and T1-weighted images were co-registered and lesion maps were drawn as overlays on the T1-weighted images guided by overlapping FLAIR images to improve contrast for accuracy.

Results

Patient classification and demographics

Healthy controls performed with 72.5% accuracy (± 8.8) and TBI patients with 64.9% (±10.5). Sensitivity index (d') scores were used to compare groups in order to account for response bias. TBI patients demonstrated significantly reduced ($t(33.1)=2.07$, $p=0.04$ SM (mean d'=0.94±0.68) for abstract art images compared to controls (mean d'=1.33±0.59). There was high heterogeneity in memory performance (d') across the patient group (control range=27.8; TBI range=42.6). We divided patients into two groups on the basis of a median split of d' scores. This produced two TBI groups with normal (NSM, n=18, mean accuracy=72.3%, mean d'=1.43(±0.59)) and impaired SM (ISM, n=17, mean accuracy=57.2%, mean d'=0.41(±0.26)). Compared to controls (CON), ISM patients were significantly impaired ($t(20.25)=5.66$, $p<0.001$) but NSM were not ($t(31.21)=-0.52$, $p=0.60$) in their SM performance (Figure 2).

< Figure 2 >

Table 1 summarises demographic data across the three groups (CON, NSM, ISM). Detailed clinical demographics for each patient are available in Supplementary material 1. Groups did not differ significantly in terms of gender or age at assessment. There was a significant difference in years of education ($F(2,37)=4.95$, $p=0.01$) with the healthy control group being more educated than the ISM group ($p<0.01$). The patient groups did not differ in age at injury, years since injury, lesion volume, PTA duration or lowest recorded GCS.

< Table 1 >

Neuropsychological performance

Widespread impairments of cognitive function were seen in ISM patients (Table 2). There were significant group effects across cognitive measures of intellectual ability ($F(2,47)=11.03$, $p<0.001$), processing speed ($F(2,47)=9.74$, $p<0.001$), executive function ($F(2,47)=6.33$,$p=0.004$), verbal memory (immediate: $F(2,26)=7.114$, $p=0.003$ and delayed: $F(2,26)=11.53$,$p<0.001$), associative memory (immediate: $F(2,47)=4.803$, $p=0.013$ and delayed: $F(2,47)=7.10$, $p=0.002$) and visuospatial memory (immediate:

F(2,26)=15.36, p<0.001 and delayed: F(2.26)=9.11, p=0.001). There was no difference between groups in measures of premorbid intelligence (F(2,26)=2.513, p=0.09).

These group effects were driven primarily by impairments in the ISM group relative to controls (Figure 2). ISM patients showed impairments in intellectual ability (p<0.001), processing speed (p<0.001) executive function(p=0.005), and verbal (immediate (p=0.003); delayed (p=<0.001)), associative (immediate (p=0.017); delayed (p=0.004)) and visuospatial memory (immediate (p<0.001); delayed (p=0.001)) compared to healthy controls. ISM patients were also impaired relative to NSM in intellectual ability (p=0.005), executive function (p=0.011), associative memory (immediate (p=0.017); delayed (p=0.004) and visuospatial memory (immediate (p<0.001); delayed (p=0.006). In contrast, NSM patients were impaired compared to controls only in processing speed (p=0.003).

Successful encoding is associated with activation changes in the dorsal attention network and default mode network

Across all participants combined, successfully remembering items (remembered minus forgotten contrast) showed higher activation bilaterally in the inferior frontal gyrus, fusiform gyrus, superior parietal lobe, IPS, lateral occipital cortex, posterior parahippocampal gyrus (PHG) and left amygdala (shown in red-yellow in Figure 3A). These regions largely fall within the DAN and MTL. Decreased activation was seen during successfully remembered items in the posterior cingulate cortex, precuneus, medial prefrontal cortex, inferior parietal lobe, superior frontal gyrus, and right medial frontal gyrus (shown in blue-light blue, Figure 3A), regions largely falling within the DMN. These patterns of activation are also sustained in the TBI group alone (Supplementary materials, Figure 1).

< Figure 3 >

TBI patients with memory impairment show differential activation during successful encoding

When comparing activation patterns in TBI patients with and without episodic memory impairment, higher-level contrasts (*NSM>ISM* and *ISM>NSM*) revealed significant

group differences during successful encoding (remembered minus forgotten). NSM showed greater activation than ISM in right precuneus, right intraparietal sulcus, left inferior temporal gyrus and bilaterally in the temporal-occiptial fusiform cortex, PHG and lingual gyrus (red-yellow in Figure 3B). All TBI patients combined did not show differential activation to controls in either direction.

In order to further explore how activation in this region related to healthy controls, and thus interpret this result in TBI patients, we extracted BOLD signal from the peak of the largest cluster (MNI:26,-80,44) of the *NSM>ISM* contrast. NSM showed a trend ($t(30.4)=-1.80$, $p=0.08$) towards greater activation than controls during successful encoding (Figure 3C) but did not differ during unsuccessful trials. Activation change did not differ between ISM TBI and controls during either successfully or unsuccessfully encoded trials in this region. Neither patient group demonstrated differential patterns of encoding compared to controls on a whole-brain voxel-wise level in either direction (i.e. *NSM >/< CON* and *ISM >/< CON* contrasts).

ISM patients showed significantly greater change in activation in left anterior prefrontal cortex spanning superior and middle frontal gyri compared to NSM during successful encoding (remembered minus forgotten; blue-light blue in Figure 3B). In the peak of this cluster (MNI:-34,52,18), ISM showed increased activation compared to controls ($t(30.5)= -2.05$, $p= 0.05$) during successfully encoded trials (Figure 3C). No difference was observed in these patients compared to controls in unsuccessful trials. NSM did not differ from controls in terms of BOLD activation in this cluster for either trial type. BOLD signal was not associated with motion, education or time since injury in either the NSM > ISM or the ISM > NSM cluster.

Patients with impaired subsequent memory show reduced white matter integrity

Next we investigated whether differences in SM impairment amongst TBI patients were associated with underlying white matter abnormalities. Voxel-wise contrasts between groups on the skeletonised white matter revealed that TBI patients in the ISM group showed significantly reduced FA compared to the NSM group in tracts including the inferior fronto-occipital fasciculus, corticospinal tracts, fornix and corpus callosum

(Figure 4A). To provide a tract level description of the data we extracted mean FA from the body, genu and splenium of the corpus callosum, and bilaterally from the cingulum, corticospinal tract, inferior fronto-occipital fasciculus and inferior and superior longitudinal fasciculi (Figure 4B). These six white matter tracts were selected as they are large enough to allow for robust sampling and less vulnerable to partial volume effects than smaller tracts. There were significant differences in FA across group ($F(2)=120.98$, $p<0.0001$) and tract ($F(12)=179.09$, $p<0.0001$). There was no interaction effect between group and tract ($p=0.09$). Mean whole-brain FA was significantly reduced in ISM compared to NSM ($p=0.04$). Both patient groups independently demonstrated significantly reduced mean whole-brain FA compared to controls ($p=0.001$).

< Figure 4 >

Patients with impaired subsequent memory show reduced connectivity in structural connectomes underpinning task-derived functional networks

We next investigated structural connectivity within the memory network modulated by memory encoding. In the white matter networks derived from activated and deactivated memory networks (Encoding activation/Encoding deactivation) during successful encoding, ISM patients showed significantly reduced structural connectivity (Encoding activation: $F(1)=6.05$, $p=0.01$; Encoding deactivation: $F(1)=6.73$, $p=0.01$) on average across the whole network compared to NSM patients (Figure 5). The effect of age and its potential interaction with group assessed and there was no significant effect of age on FA in either network (Encoding activation($F(1)=1.61$, $p=0.21$; Encoding deactivation: $F(1)=2.51$, $p=0.12$), nor any interaction between group and age in the Encoding activation($F=0.864$, $p=0.361$) or Encoding deactivation ($F=1.25$, $p=0.272$) networks.

ISM showed reduced FA in white matter underpinning the structural connectivity between right pericalcarine cortex and left insula ($p=0.032$, $z=3.49$) derived from the Encoding activation network, compared to NSM. In the encoding deactivation network ($p=0.034$), structural connectivity was reduced between right accumbens area and right supramarginal gyrus ($z=3.11$), left caudal middle frontal gyrus and left superiorfrontal

gyrus (z= 3.18) and left precuneus and left rostral middle frontal gyrus (z=3.98) in ISM compared to NSM (Figure 5).

< Figure 5 >

Lesions

Focal lesions were present in 10 NSM and 7 ISM patients (Figure 6). No lesions overlapped any significant clusters within the *NSM>ISM* contrast. The significant cluster within the *ISM>NSM* contrast overlapped with lesioned voxels in 3 ISM and 4 NSM patients. Removal of these subjects did not diminish the effect of reduced BOLD activation in the ISM compared to the NSM patients ($t(27.99)=-2.87$, $p=0.008$) during correctly encoded trials within this cluster.

< Figure 6 >

Motion

Motion across all participants was minimal with FD measures averaging 0.13mm across all subjects. This varied slightly across groups ($F(2,48)=3.23$, $p<0.05$) with more movement (uncorrected $p<0.05$) in the ISM group (mean=0.14, SD=0.07) compared to controls (mean=0.1, SD=0.03), however this did not survive multiple comparisons correction (FDR corrected $p=0.06$). Removal of noise components using ICA-AROMA did not differ between groups ($F(2,48)=0.77$, $p=0.47$), with 50% of resulting components being removed on average across all subjects (NSM=51%, ISM=52%, Controls=47%).

Discussion

Episodic memory impairment is common following TBI but the neural basis for this is unclear. Our results show for the first time that TBI patients with impaired episodic memory show abnormal activation of memory networks during successful encoding compared to patients with normal memory function. The results provide novel insights into the mechanisms underlying episodic memory impairment within the TBI population. Abnormal activation of key nodes within the DAN and regions regulating DMN activity during encoding are predictive of subsequent retrieval. We demonstrate a clear relationship between functional networks activated during encoding and underlying structural abnormalities in patients with memory impairment and suggest that encoding failures in this group are likely due to failed control of attentional resources.

Successful memory encoding is normally associated with activation of a range of brain regions including extensive parts of the DAN and MTL (Kim, 2011, 2015). In contrast, subsequently forgetting is associated with greater activation in DMN regions (Kim, 2011). Our results across all participants combined were largely in keeping with these findings and suggest that activation of the DAN and suppression of the DMN is required for successful encoding.

Activation of the DAN is thought to be crucial for stimulus directed attention (Majerus *et al.*, 2018). The right IPS, a key hub in the DAN, is particularly important because of its involvement in the mediation of goal-directed 'top-down' attention. Activation of IPS has been consistently associated with successful encoding and it has been proposed that allocating goal-directed attention during encoding increases the probability of retrieval (Uncapher and Wagner, 2009). Patients with intact memory performance showed greater activation than impaired patients in right IPS. This might be the result of compensatory recruitment of DAN regions that improves cognitive function, specifically attentional control, while ISM TBI patients are not able to utilise this mechanism. Previous work has demonstrated hyperactivation in a range of brain regions during letter encoding in TBI patients, in the absence of behavioural differences to controls (Russell *et al.*, 2011; Arenth *et al.*, 2012). These results are difficult to interpret because contrasts were between stimuli encoding conditions (e.g. picture

versus word) and the lack of behavioural deficits in the TBI group means observed increased activation cannot be associated with cognitive performance. The direct comparison of patients with and without memory impairment here clarifies that increased activation of these regions during memory encoding is likely to be compensatory.

In addition, we show that activation in the PHG bilaterally is decreased in TBI patients with episodic memory impairment. This region has consistently been associated with increased activation during successful encoding (Dove *et al.*, 2006; Kim, 2011). The PHG, a key node in the DMN, is thought to act as a link between the MTL memory system and the cortical nodes of the DMN (Ward *et al.*, 2014). Functional connectivity between MTL and DMN has been associated with memory encoding (Huijbers *et al.*, 2011) and we have previously shown that patients in post-traumatic amnesia after TBI have abnormal functional connectivity between PHG and DMN (De Simoni *et al.*, 2016). Here we provide further evidence that abnormalities of PHG function are an important determinant of memory function after TBI.

Memory impairments were associated with increased activity in the left anterior prefrontal cortex (aPFC). There are a number of potential reasons why aPFC activation is higher in patients with memory impairment. The region is thought to be involved in the processing of internal mental states and mind-wandering (Christoff and Gabrieli, n.d.), and the transition between brain resting state and task-processing state (Peng *et al.*, 2018). One hypothesis is that activation of this region is high because patients that engaged in mind-wandering or with internally focused attention show poorer encoding of memory. The aPFC is thought to exert suppressive top-down control over the DMN to facilitate goal-directed behaviours, and procrastination or mind-wandering occurs when this control is lost (Zhang *et al.*, 2016).

An alternative explanation is that the increased activity is a compensatory response to greater cognitive load during attempted memory encoding. Memory impairment associated with healthy ageing has been associated with increased PFC recruitment in older adults (Dennis *et al.*, 2007). Taken with findings that show PFC-MTL connectivity is altered in ageing, it has been suggested that ‘over-activation’ of PFC in older adult populations could reflect functional compensation for dysfunction within

the MTL system(Nyberg, 2017). Here, we have shown increased aPFC activation in TBI patients with SM impairment which may be reflective of compensatory processes as described in the healthy ageing literature.

Consistent with this compensatory hypothesis is the direction of change in the BOLD signal extracted from the peak of the aPFC cluster (Figure 3C). In TBI patients with normal subsequent memory performance, the direction of signal change is the same as for controls, though exaggerated, suggesting this 'extra' suppression is required for TBI patients without overt mnemonic impairment to encode successfully. In TBI patients with impaired memory however the signal change is in the opposite direction suggesting that encoding in those with mnemonic deficits may be fundamentally altered, either through recruitment of additional resources or a functional reorganisation. Reorganisation of functional networks following brain injury can be associated with cognitive changes (Warren *et al.*, 2009; Ainsworth *et al.*, 2018). It is therefore possible that functional reorganisation within networks involved in memory function might explain the patterns of abnormal activation seen here.

Impaired SM was associated with reduced integrity of white matter microstructure. In keeping with these findings, a previous study found that successful learning was associated with higher FA values in the forceps, fronto-occipital fasciculus and thalamic radiation (Chiou *et al.*, 2016). Previous work from our group showing the association between reduced white matter integrity in the fornix and impaired associative learning and memory is also consistent with the present findings of reduced structural connectivity and cognitive impairments (Kinnunen *et al.*, 2011). Taken together with our functional imaging findings, this suggests that normal functional activation during memory encoding is reliant on structural white matter integrity.

To explore this hypothesis further we examined the underlying white matter architecture of the functional encoding networks and showed significantly reduced connectivity in both encoding activation and encoding deactivation networks associated with memory impairment. The tracts used to define these structural networks represent tractography derived connectivity between grey matter regions, and so while these structural networks do not represent traditional anatomical tracts, they do allow a more detailed investigation of the relationship between structural and functional networks.

The strongest effect was found in white matter underpinning connections between left precuneus and rostral middle frontal gyrus, core nodes within the DMN. The precuneus, in healthy cognition, interacts with both DMN and frontoparietal networks to engage in different cognitive states (Utevsky *et al.*, 2014). Abnormal structural connections linking a key hub of the DMN with prefrontal cortex implicated in executive control, and in this case abnormal activation in impaired memory function, suggests a potential mechanism through which structural damage underpins cognitive deficits. We have previously shown that DMN connectivity predicts variability in sustained attention impairment within a TBI population (Bonnelle *et al.*, 2011), which is consistent with the current findings. Furthermore, within the encoding deactivation network, all connections that showed significantly reduced integrity of the underlying white matter microstructure had connections to/from nodes that overlapped with the encoding activation network. This would suggest that communications not only within the encoding deactivation network, but also between encoding activation and deactivation networks, is associated with impaired memory in TBI. This evidence is in-keeping with memory impairment arising as the result of failure to appropriately engage and disengage functional networks modulating attentional control as a consequence of damage to the underlying white matter microstructure.

Some potential limitations should be considered. An important consideration in any functional imaging study is that of subject movement. Very small amounts of motion were seen in our patients, and motion metrics did not differ between groups. We therefore do not think this is a factor in explaining our results. Nevertheless, we took a number of steps in order to ensure that physiological motion artefact was accounted for during data analysis including removal of subjects with larger degrees of motion and decomposing the data to eliminate components largely consisting of motion. Another limitation is the potential effect that educational level could have on the behavioural results given the memory impaired patients were less educated than healthy controls. Recent meta-analysis suggested higher educational level is associated with improved visuospatial recall and better recovery (Vakil *et al.*, 2019). However, there was no difference in educational levels between the ISM and NSM TBI groups and we do not therefore think this should change the interpretation of the results. Caution must be taken when extrapolating a failure to encode from the current paradigm, as no robust measure of attention was employed. In order to ensure that images are attended to

during the encoding phase, a simple judgement task could be utilised. The effects of not having this in place would have led to mind wandering and this would be interpreted as a failure to attend than a failure to encode. The deficit in these patients could therefore be representing a fundamental failure in memory, or of, as we have suggested above, a failed control of attentional resources. In terms of lesions, the pattern of focal cortical damage we observed cannot explain our functional imaging results, as the difference in BOLD activation in areas overlapped by such damage between the ISM and NSM TBI groups remained significant when patients with lesions in those areas were removed from the analysis. Finally, the use of a separate independent control group for the structural imaging limits the ability to assess the relationship between our functional and structural encoding networks in a control population, however given the focus here was to understand underlying mechanisms of mnemonic deficits within the TBI population, this did not impair our ability to explore the differences between ISM and NSM patients.

An interesting future direction would be to estimate the relative contributions of fMRI, diffusion MRI and lesion location to individual variability in memory performance, which could be achieved using approaches such as the Pattern Recognition for Neuroimaging Toolbox (PRONTO; (Schrouff *et al.*, 2013)). Another direction would be to investigate longitudinal changes in brain structure. Brain atrophy can progress following TBI and these changes predict cognitive function (Cole *et al.*, 2015). Progressive atrophy after TBI is indicative of neurodegeneration and the relationship between this progressive process and memory function could be quantified using longitudinal assessment of brain volumes

Understanding the abnormalities of brain network function associated episodic memory failure after TBI creates opportunity for potential therapeutic intervention. Brain stimulation using transcranial direct-current stimulation (tDCS), transcranial magnetic stimulation (TMS) and deep brain stimulation (DBS) provide opportunities to modulate brain activity and potentially improve memory function after TBI. We have previously shown that tDCS can improve executive function, an effect that is influenced by the underlying structural connectivity of the stimulated network in healthy individuals and patients after TBI (Li *et al.*, 2019*a*, *b*). The results we present inform the choice of future stimulation studies aimed at enhancing memory function. TBI patients with

intact memory performance showed greater activation than impaired patients in right IPS, perhaps due to compensatory recruitment of the DAN. This leads to the prediction right IPS stimulation during memory encoding may normalise memory impairments after TBI by increasing DAN activity. This region is accessible to non-invasive brain stimulation, which might be achieved through the use of TDCS. However, more focal brain stimulation could be needed, achieved non-invasively with TMS or invasively through DBS, which could become an option in the future. Future work should quantify abnormalities of structural connectivity within white matter tracts connecting memory network nodes, as this is likely to influence the response to brain stimulation (Li *et al.*, 2019*b*)

In summary, TBI patients with SM impairment show dissociable functional and structural abnormalities from those with normal SM performance. Our results demonstrate a clear relationship between abnormal activation of functional networks during encoding and damage to the underlying structural connectivity of these networks.

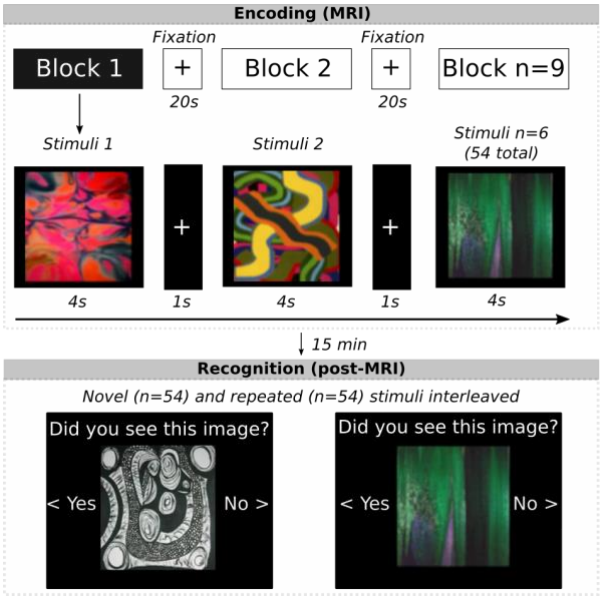

Figure 1. The subsequent memory task paradigm consisting of an in-scanner encoding task and a post-scanner recognition task.

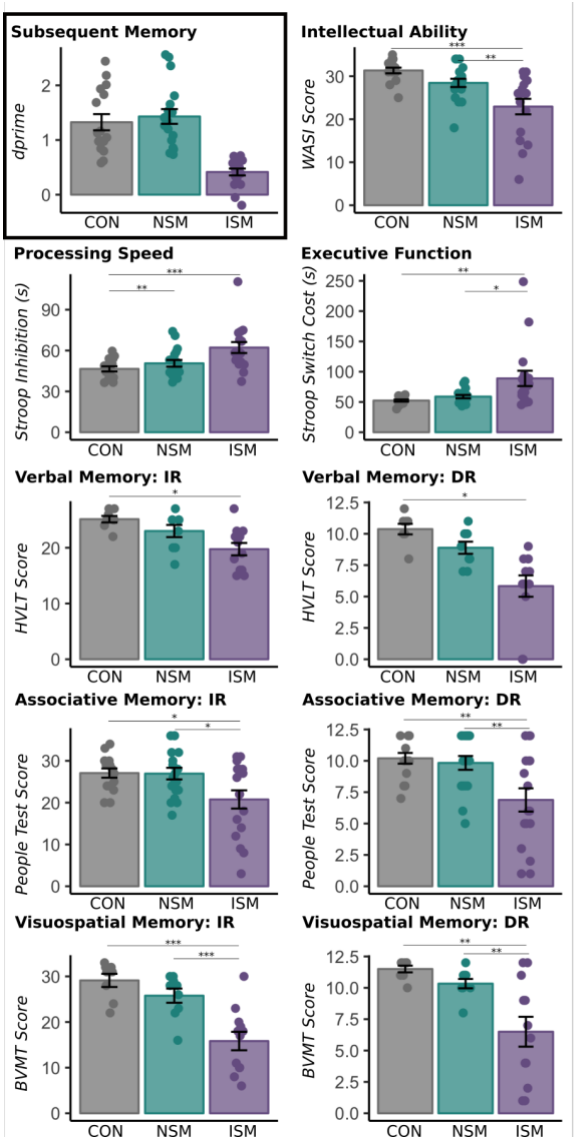

Figure 2. Performance on the post-scanner recognition task and standardised neuropsychological assessment in TBI patients split into normal subsequent memory (NSM)and impaired subsequent memory (ISM) groups, and healthy controls.. *** $p < 0.001$; ** $p<0.01$; * $p<0.05$

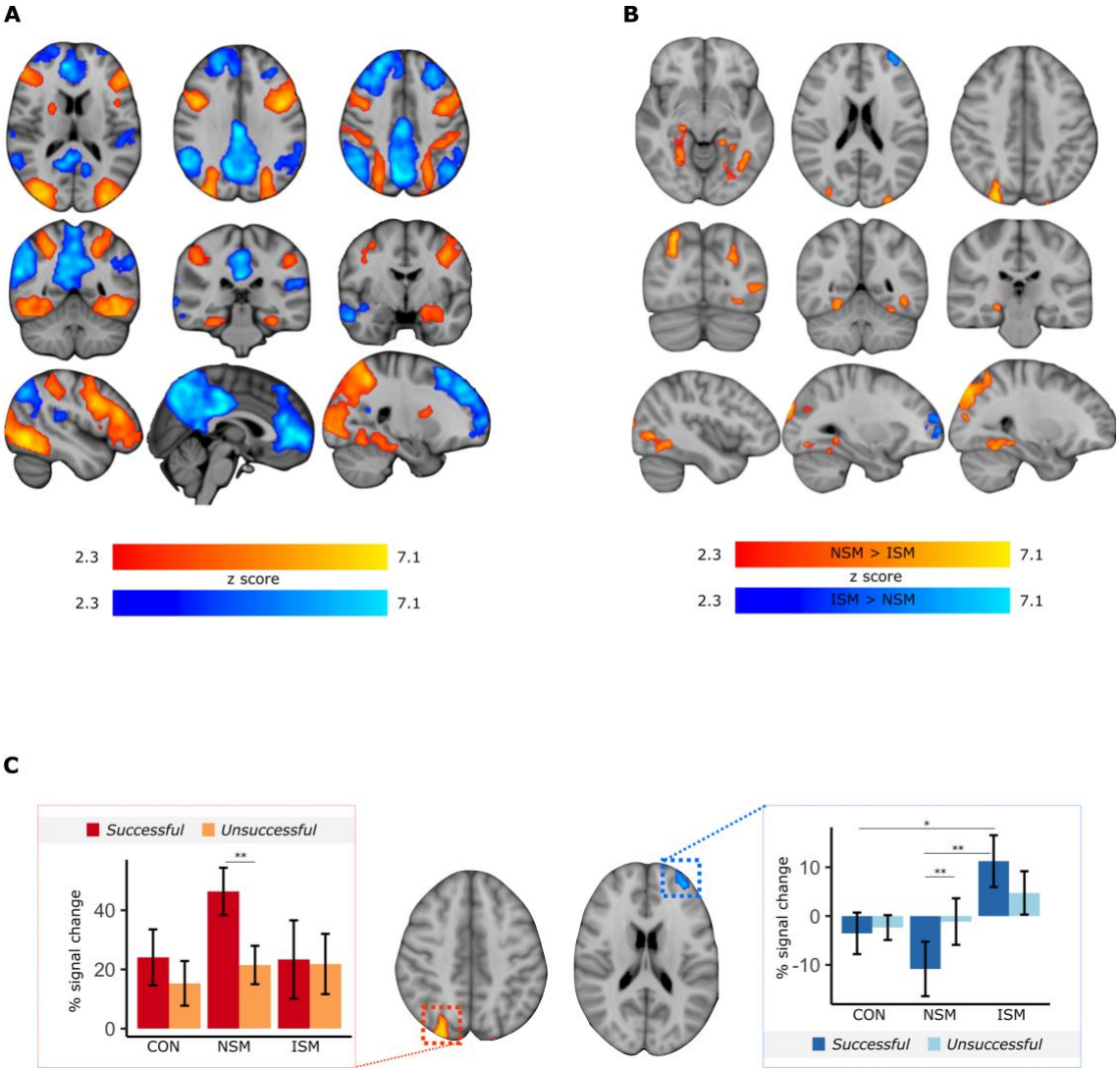

Figure 3. Alterations in BOLD activity associated with performance on the memory encoding task. All spatial results shown in standard space overlaid on MNI template with a Z-statistic threshold of 2.3. **A.** All subjects. Voxels showing increased activation during successful encoding (remembered minus forgotten contrast) in red-yellow and decreased activation in blue-light blue. **B.** Contrasts between TBI patient groups. Voxels in which patients with normal subsequent memory showed greater increases in activation during successful encoding compared to patients with impaired subsequent memory (NSM > ISM contrast) shown in red-yellow. Voxels in which patients with impaired subsequent memory show greater decreases in activation during successful encoding compared to patients with normal subsequent memory (ISM > NSM contrast) shown in blue-light blue. **C.** Percentage change in BOLD signal across groups in successful and unsuccessful encoding in the peak of the NSM > ISM cluster (left) and the ISM > NSM cluster (right).

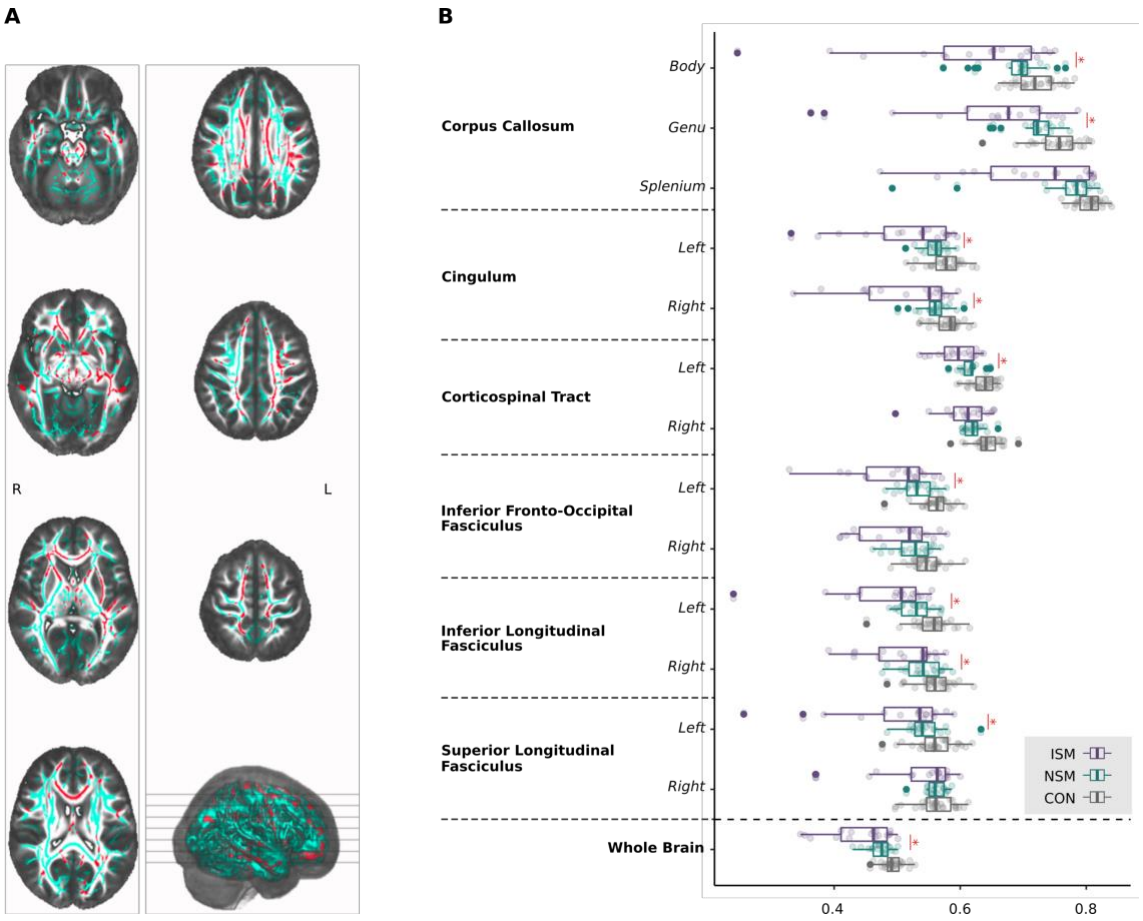

Figure 4. A. TBI patients with subsequent memory impairment showed significantly reduced FA (shown in red) compared to TBI patients with normal subsequent memory. TFCE corrected results ($p < 0.05$) shown overlaid on the mean FA skeleton (cyan). **B.** Mean FA across individual white matter tracts and whole brain for each group.

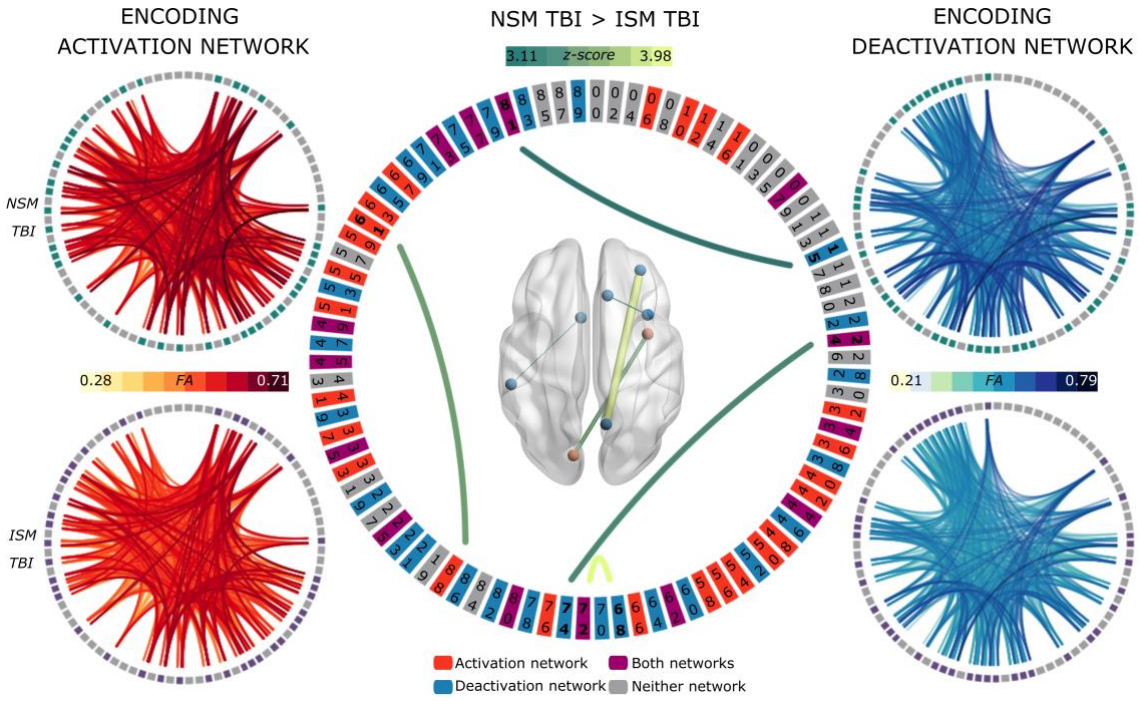

Figure 5. Structural connectome underlying the positive (red) and negative (blue) encoding networks in NSM (top row) and ISM TBI (bottom row) patients are shown in the outer circles. ISM TBI patients showed reduced structural connectivity between nodes within the positive (p=0.032) and negative (p=0.034) networks. Corresponding labels from the Deskian-Killianey grey matter parcellation scheme with significantly different connections as shown on the innermost circle are as follows: **15.** Right-Accumbens-area; **24**. ctx-lh-caudalmiddlefrontal; **61**. ctx-rh-pericalcalcarine; **68**. ctx-lh-precuneus; **72**. ctx-lh-rostralmiddlefrontal; **74**. ctx-lh-superiorfrontal; **81**. ctx-rh-supramarginal; **88**. ctx-lh-insula

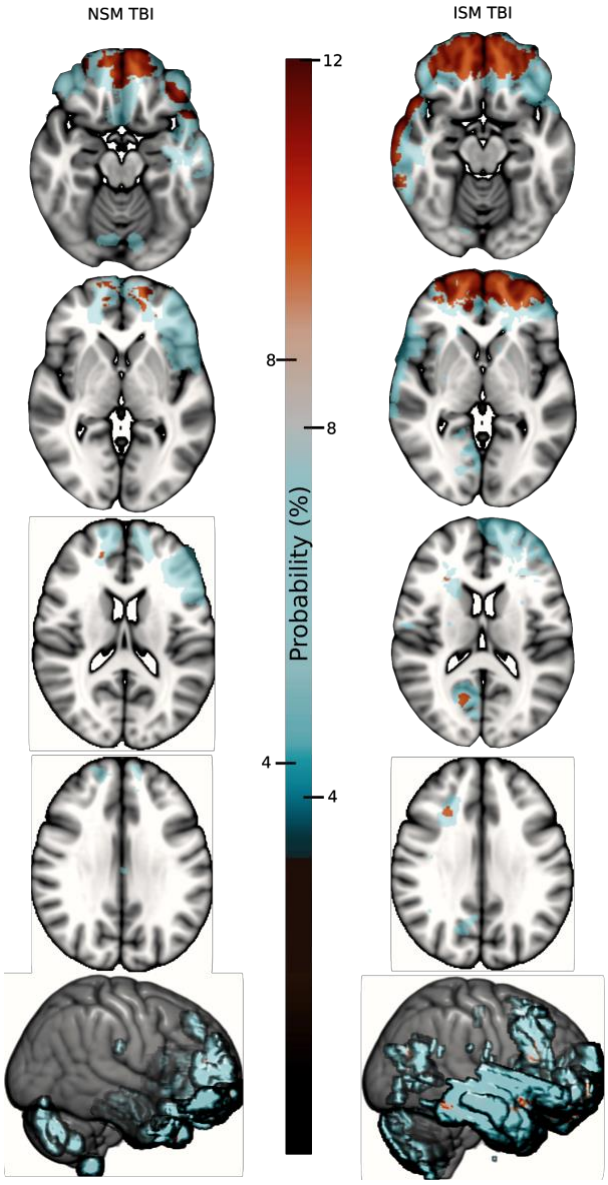

Figure 6. Lesion probability maps for TBI patients with normal subsequent memory (left) and TBI patients with impaired subsequent memory (right) indicating, for every voxel, the lesion frequency within the respective patient samples.

Table 1. Demographics

	CON n= 16		NSM n= 18		ISM n= 17		Statistic	*p*	Post-hoc group differences[†]
Gender	6F:10M		4F:14M		5F:12M		$X^2 = 0.95$	0.62	-
	Mean	*SD*	*Mean*	*SD*	*Mean*	*SD*			
Age	38.19	11.99	39.89	9.28	46.71	12.24	F = 2.72	0.08	-
Years of Education	18.21	3.87	16.08	2.84	13.77	4.15	F = 6.25	0.01	CON > ISM**
Age at Injury	-	-	33.39	11.64	31.71	14.7	t = 0.37	0.71	-
Time Since Injury (months)	-	-	80.12	104.03	176.18	192.61	t =-1.82	0.08	-
Lesion Volume (voxels)	-	-	14023	18513	24282	36578.66	t=-1.04	0.31	
PTA Duration (days)	-	-	14.6	23.87	22.69	36.89	t=-0.68	0.51	
Lowest GCS	-	-	6.15	4.91	7.22	4.35	t=-0.54	0.60	

** $p < 0.01$; [†]false discovery rate corrected for multiple comparisons; CON = Controls; ISM = impaired subsequent memory TBI patients; NSM = normal subsequent memory TBI patients

Table 2. Neuropsychological performance

Cognitive Domain	Neuropsychological test	CON Mean (± SD) *n* = 16	NSM Mean (± SD) *n* = 18	ISM Mean (± SD) *n* = 17	*F*	*p*	Post-hoc group differences†
Processing speed	Trail Making Test A (s)	20.11 (5.72)	22.51 (6.74)	38.86 (19.54)	10.99	< 0.001	ISM > CON*** ISM > NSM***
	Trail Making Test B (s)	45.47 (11.22)	55.69 (23.31)	85.02 (50.56)	6.18	0.004	ISM > CON** ISM > NSM*
	Stroop Colour Naming and Word Reading Composite Score (s)	31.65 (6.30)	40.85 (7.28)	44.01 (10.23)	9.74	< 0.001	ISM > CON*** NSM > CON**
Executive function	Trail Making Test B-A (s)	25.46 (9.18)	33.12 (20.05)	46.16 (35.96)	2.87	0.066	
	Stroop Inhibition (s)	46.52 (7.39)	50.61 (10.57)	62.19 (16.6)	7.19	0.002	ISM > CON** ISM > NSM*
	Stroop Inhibition-Switching (s)	52.34 (6.76)	58.89 (11.58)	88.91 (52.30)	6.33	0.004	ISM > CON** ISM > NSM*
	Stroop Inhibition-Switching versus Baseline Contrast (s)	25.29 (13.66)	20.18 (11.54)	46.79 (46.67)	4.04	0.024	ISM > NSM*
Intellectual ability	WTAR Scaled	112.53 (9.46)	106.44 (15.42)	100.38 (18.59)	2.51	0.092	
	WASI Matrix Reasoning	31.33 (2.55)	28.44 (4.08)	22.94 (7.43)	11.03	< 0.001	CON > ISM*** NSM > ISM**
Verbal memory	WMS-III LM Immediate Recall	48.77 (7.58)	44.35 (9.99)	37.2 (9.73)	4.48	0.012	CON > ISM*
	WMS-III LM Delayed Recall	31.23 (5.90)	28.81 (7.90)	23.50 (7.63)	3.32	0.048	CON > ISM*
	WMS-III LM Retention	89.55 (11.84)	91.68 (13.35)	84.18 (11.77)	1.13	0.335	
	WMS-III LM Recognition	28.69 (1.44)	27.06 (2.32)	24.7 (3.59)	7.32	0.002	CON > ISM** NSM >ISM*
	WMS-III LM Learning	5.00 (3.16)	3.94 (2.38)	4.80 (2.25)	0.68	0.512	
	HVLT-R Immediate Recall	25.12 (1.64)	23 (3.28)	19.75 (3.84)	7.11	0.003	CON > ISM** NSM > ISM*
	HVLT-R Delayed Recall	10.38 (1.19)	8.89 (1.45)	5.83 (2.95)	11.53	< 0.001	CON > ISM*** NSM > ISM**
	HVLT-R Recognition	10.75 (1.04)	10.67 (1.32)	9.00 (2.59)	2.79	0.080	
Associative Memory	People's Test Immediate Recall	27.07 (4.28)	26.94 (5.88)	20.76 (8.98)	4.80	0.013	NSM > ISM* CON > ISM*
	People's Test Delayed Recall	10.20 (1.66)	9.83 (2.33)	6.88 (3.82)	7.10	0.002	CON > ISM** NSM > ISM**
	People's Test Forgetting	1.53 (1.41)	1.61 (1.91)	2.71 (2.47)	1.80	0.177	
Visuospatial memory	BVMT-R Immediate Recall	29.12 (4.09)	25.78 (4.66)	15.83 (7.0)	15.36	< 0.001	CON > ISM*** NSM > ISM***
	BVMT-R Delayed Recall	11.50 (0.76)	10.33 (1.12)	6.50 (4.12)	9.11	<0.001	CON > ISM** NSM > ISM**
	BVMT-R Recognition	5.75 (0.46)	5.56 (0.88)	4.67 (1.97)	1.79	0.188	

* p < 0.05; ** p< 0.01; *** p < 0.001; † false discovery rate corrected for multiple comparisons; **BVMT-R** = Brief Visuospatial Memory Test-Revised; **CON** = controls; **HVLT-R** = Hopkins Verbal Learning Test-Revised; **ISM** = impaired subsequent memory TBI patients ; **NSM**= normal subsequent memory TBI patients; **SD** = standard deviation; **WASI** = Wechsler Abbreviated Scale for Intelligence; **WMS-III** = Wechsler Memory Scale, Third Edition; **WTAR** = Wechsler Test of Adult Reading

Glossary

TBI Traumatic brain injury

BOLD Blood oxygenation level dependent

DTI diffusion tensor imaging

FA fractional anisotropy

SM subsequent memory

DMN default mode network

DAN dorsal attention network

ISM impaired subsequent memory

NSM normal subsequent memory

Acknowledgements and Funding

We would like to thank the patients with traumatic brain injury and the healthy controls who gave their time to participate in this study.

EM is supported by a National Institute of Health Research (NIHR) Invention for Innovation (i4i) Research Award (II-LB-0715-20006) awarded to DJS and AH. GS is supported by NIHR. LML is supported by a Wellcome Trust Clinical Research Training Fellowship (103429/Z/13/Z). SAGR is supported by a Royal College of Surgeons (RCSEng) Military Surgical Research Fellowship and the Ministry of Defence. AH is supported by the UK Dementia Research Institute and NIHR. DJS is supported by an NIHR Professorship (NIHR-RP-011-048), the NIHR Clinical Research Facility and Biomedical Research Centre at Imperial College Healthcare NHS Trust & The Royal British Legion Centre for Blast Injury Studies.

Author contributions
Study concept and design: AH and DJS
Data acquisition and analysis: EM, SD, GS, AEJ, LML, NJB, SAGR and NG
Drafting manuscript and figures: EM and DJS

Conflicts of Interest

There are no conflicts of interest to report.

References

Ainsworth M, Browncross H, Mitchell DJ, Mitchell AS, Passingham RE, Buckley MJ, et al. Functional reorganisation and recovery following cortical lesions: A preliminary study in macaque monkeys. Neuropsychologia 2018; 119: 382–391.

Arenth PM, Russell KC, Scanlon JM, Kessler LJ, Ricker JH. Encoding and recognition after traumatic brain injury: neuropsychological and functional magnetic resonance imaging findings. J Clin Exp Neuropsychol 2012; 34: 333–44.

Baddeley AD, Emslie H, Nimmo-Smith I. Doors and People: A Test of Visual and Verbal Recall and Recognition, Thames Valley Test Company, Bury St. Edmunds, UK 1994

Bonnelle V, Ham TE, Leech R, Kinnunen KM, Mehta MA, Greenwood RJ, et al. Salience network integrity predicts default mode network function after traumatic brain injury. Proc Natl Acad Sci 2012; 109: 4690–4695.

Bonnelle V, Leech R, Kinnunen KM, Ham TE, Beckmann CF, De Boissezon X, et al. Default Mode Network Connectivity Predicts Sustained Attention Deficits after Traumatic Brain Injury. J Neurosci 2011; 31: 13442–13451.

Catani M, Thiebaut De Schotten M. A diffusion tensor imaging tractography atlas for virtual in vivo dissections. Cortex 2008; 44: 1105–32.

De Chastelaine M, Mattson JT, Wang TH, Donley BE, Rugg MD. Sensitivity of negative subsequent memory and task-negative effects to age and associative memory performance. Brain Res 2015; 1612: 16–29.

Chiou KS, Genova HM, Chiaravalloti ND. Structural white matter differences underlying heterogeneous learning abilities after TBI. Brain Imaging Behav 2016; 10: 1274–1279.

Christoff K, Gabrieli JDE. The frontopolar cortex and human cognition: Evidence for a rostrocaudal hierarchical organization within the human prefrontal cortex. Psychobiology; 28: 168–186.

Cole JH, Leech R, Sharp DJ. Prediction of brain age suggests accelerated atrophy after traumatic brain injury. Ann Neurol 2015; 77: 571–581.

Corporation TP. Manual for the Wechsler Abbreviated Scale of Intelligence. 1999

Criminisi A, Sharp T, Blake A. GeoS: Geodesic Image Segmentation. In: Forsyth D, Torr P, Zisserman A, editor(s). Computer Vision -- ECCV 2008. Berlin, Heidelberg: Springer Berlin Heidelberg; 2008. p. 99–112

Daselaar SM, Prince SE, Dennis NA, Hayes SM, Kim H, Cabeza R. Posterior midline and ventral parietal activity is associated with retrieval success and encoding failure. Front Hum Neurosci 2009; 3

Delis DC, Kaplan E, Kramer JH. Delis-Kaplan executive function system (D-KEFS). Psychological Corporation; 2001

Dennis NA, Daselaar S, Cabeza R. Effects of aging on transient and sustained successful memory encoding activity. Neurobiol Aging 2007; 28: 1749–58.

Desikan RS, Ségonne F, Fischl B, Quinn BT, Dickerson BC, Blacker D, et al. An automated labeling system for subdividing the human cerebral cortex on MRI scans into gyral based regions of interest. Neuroimage 2006; 31: 968–980.

Dove A, Brett M, Cusack R, Owen AM. Dissociable contributions of the mid-ventrolateral frontal cortex and the medial temporal lobe system to human memory. Neuroimage 2006; 31: 1790–1801.

Gillis MM, Hampstead BM. A two-part preliminary investigation of encoding-related activation changes after moderate to severe traumatic brain injury: hyperactivation, repetition suppression, and the role of the prefrontal cortex. Brain Imaging Behav 2015; 9: 801–820.

Griffanti L, Douaud G, Bijsterbosch J, Evangelisti S, Alfaro-Almagro F, Glasser MF, et al. Hand classification of fMRI ICA noise components. Neuroimage 2017; 154: 188–205.

Himanen L, Portin R, Isoniemi H, Helenius H, Kurki T, Tenovuo O. Longitudinal cognitive changes in traumatic brain injury: A 30-year follow-up study. Neurology 2006; 66: 187–192.

Huijbers W, Pennartz CMA, Cabeza R, Daselaar SM. The Hippocampus Is Coupled with the Default Network during Memory Retrieval but Not during Memory Encoding. PLoS One 2011; 6: e17463.

Jenkinson M, Bannister P, Brady M, Smith S. Improved optimization for the robust and accurate linear registration and motion correction of brain images. Neuroimage 2002; 17: 825–41.

Jilka SR, Scott G, Ham T, Pickering A, Bonnelle V, Braga RM, et al. Damage to the Salience Network and Interactions with the Default Mode Network. J Neurosci 2014; 34: 10798–10807.

Kim H. Neural activity that predicts subsequent memory and forgetting: A meta-analysis of 74 fMRI studies. Neuroimage 2011; 54: 2446–2461.

Kim H. Encoding and retrieval along the long axis of the hippocampus and their relationships with dorsal attention and default mode networks: The HERNET model. Hippocampus 2015; 25: 500–510.

Kinnunen KM, Greenwood R, Powell JH, Leech R, Hawkins PC, Bonnelle V, et al. White matter damage and cognitive impairment after traumatic brain injury. Brain 2011; 134: 449–63.

Li LM, Violante IR, Leech R, Hampshire A, Opitz A, McArthur D, et al. Cognitive enhancement with Salience

Network electrical stimulation is influenced by network structural connectivity. Neuroimage 2019; 185: 425–433.
Li LM, Violante IR, Zimmerman K, Leech R, Hampshire A, Patel M, et al. Traumatic axonal injury influences the cognitive effect of non-invasive brain stimulation. Brain 2019; 142: 3280–3293.
Majerus S, Péters F, Bouffier M, Cowan N, Phillips C. The dorsal attention network reflects both encoding load and top-down control during working memory. J Cogn Neurosci 2018; 30: 144–159.
Malec JF, Brown AW, Leibson CL, Flaada JT, Mandrekar JN, Diehl NN, et al. The Mayo Classification System for Traumatic Brain Injury Severity. J Neurotrauma 2007; 24: 1417–1424.
Mori S (Susumu), Crain BJ. MRI atlas of human white matter. Elsevier; 2005
Nyberg L. Functional brain imaging of episodic memory decline in ageing. J Intern Med 2017; 281: 65–74.
Peng K, Steele SC, Becerra L, Borsook D. Brodmann area 10: Collating, integrating and high level processing of nociception and pain. Prog Neurobiol 2018; 161: 1–22.
Power JD, Barnes KA, Snyder AZ, Schlaggar BL, Petersen SE. Spurious but systematic correlations in functional connectivity MRI networks arise from subject motion. Neuroimage 2012; 59: 2142–54.
Pruim RHR, Mennes M, van Rooij D, Llera A, Buitelaar JK, Beckmann CF. ICA-AROMA: A robust ICA-based strategy for removing motion artifacts from fMRI data. Neuroimage 2015; 112: 267–277.
Reitan RM. Validity of the Trail Making Test as an indicator of organic brain damage. Percept Mot Skills 1958; 8: 271–276.
Ricker JH, Chugani H, Mller R-A, Zafonte RD, Black KM, Millis SR. Verbal Recall and Recognition Following Traumatic Brain Injury: A [O-15]-Water Positron Emission Tomography Study. J Clin Exp Neuropsychol (Neuropsychology, Dev Cogn Sect A) 2001; 23: 196–206.
Russell KC, Arenth PM, Scanlon JM, Kessler LJ, Ricker JH. A functional magnetic resonance imaging investigation of episodic memory after traumatic brain injury. J Clin Exp Neuropsychol 2011; 33: 538–47.
Schrouff J, Rosa MJ, Rondina JM, Marquand AF, Chu C, Ashburner J, et al. PRoNTo: Pattern recognition for neuroimaging toolbox. Neuroinformatics 2013; 11: 319–337.
Sharp DJ, Beckmann CF, Greenwood R, Kinnunen KM, Bonnelle V, De Boissezon X, et al. Default mode network functional and structural connectivity after traumatic brain injury. Brain 2011; 134: 2233–2247.
De Simoni S, Grover PJ, Jenkins PO, Honeyfield L, Quest RA, Ross E, et al. Disconnection between the default mode network and medial temporal lobes in post-traumatic amnesia. Brain 2016: 1–14.
De Simoni S, Jenkins PO, Bourke NJ, Fleminger JJ, Hellyer PJ, Jolly AE, et al. Altered caudate connectivity is associated with executive dysfunction after traumatic brain injury. Brain 2018; 141: 148–164.
Smith SM. Fast robust automated brain extraction. Hum Brain Mapp 2002; 17: 143–155.
Smith SM, Jenkinson M, Johansen-Berg H, Rueckert D, Nichols TE, Mackay CE, et al. Tract-based spatial statistics: Voxelwise analysis of multi-subject diffusion data. Neuroimage 2006; 31: 1487–1505.
Smith SM, Jenkinson M, Woolrich MW, Beckmann CF, Behrens TEJ, Johansen-Berg H, et al. Advances in functional and structural MR image analysis and implementation as FSL. Neuroimage 2004; 23: S208–S219.
Strangman GE, Goldstein R, O'Neil-Pirozzi TM, Kelkar K, Supelana C, Burke D, et al. Neurophysiological Alterations During Strategy-Based Verbal Learning in Traumatic Brain Injury. Neurorehabil Neural Repair 2008; 23: 226–236.
Uncapher MR, Wagner AD. Neurobiology of Learning and Memory Posterior parietal cortex and episodic encoding : Insights from fMRI subsequent memory effects and dual-attention theory. Neurobiol Learn Mem 2009; 91: 139–154.
Utevsky A V, Smith D V, Huettel SA. Precuneus is a functional core of the default-mode network. J Neurosci 2014; 34: 932–40.
Vakil E. The Effect of Moderate to Severe Traumatic Brain Injury (TBI) on Different Aspects of Memory: A Selective Review Memory Impairment in Patients with Traumatic Brain Injury E. Vakil. J Clin Exp Neuropsychol 2005; 27: 0–0.
Vakil E, Greenstein Y, Weiss I, Shtein S. The Effects of Moderate-to-Severe Traumatic Brain Injury on Episodic Memory: a Meta-Analysis. Neuropsychol Rev 2019; 29: 270–287.
Wallace EJ, Mathias JL, Ward L. Diffusion tensor imaging changes following mild, moderate and severe adult traumatic brain injury: a meta-analysis. Brain Imaging Behav 2018; 12: 1607–1621.
Ward AM, Schultz AP, Huijbers W, Van Dijk KRA, Hedden T, Sperling RA. The parahippocampal gyrus links the default-mode cortical network with the medial temporal lobe memory system. Hum Brain Mapp 2014; 35: 1061–1073.
Warren JE, Crinion JT, Lambon Ralph MA, Wise RJS. Anterior temporal lobe connectivity correlates with functional outcome after aphasic stroke. Brain 2009; 132: 3428–3442.
Wechsler D. Wechsler memory scale (WMS-III). Psychological corporation San Antonio, TX; 1997
Wechsler D. Wechsler Test of Adult Reading: WTAR. Psychological Corporation; 2001
Wright MJ, Schmitter-Edgecombe M, Woo E. Verbal memory impairment in severe closed head injury: the role of encoding and consolidation. J Clin Exp Neuropsychol 2010; 32: 728–36.

Zalesky A, Fornito A, Bullmore ET. Network-based statistic: Identifying differences in brain networks. Neuroimage 2010; 53: 1197–1207.
Zhang H, Yushkevich PA, Alexander DC, Gee JC. Deformable registration of diffusion tensor MR images with explicit orientation optimization. Med Image Anal 2006; 10: 764–785.
Zhang S, Arfanakis K. Evaluation of standardized and study-specific diffusion tensor imaging templates of the adult human brain: Template characteristics, spatial normalization accuracy, and detection of small inter-group FA differences. Neuroimage 2018; 172: 40–50.
Zhang W, Wang X, Feng T. Identifying the Neural Substrates of Procrastination: a Resting-State fMRI Study OPEN. Nat Publ Gr 2016
Zhang Y, Brady M, Smith S. Segmentation of brain MR images through a hidden Markov random field model and the expectation-maximization algorithm. IEEE Trans Med Imaging 2001; 20: 45–57.

Supplementary Table 1. Demographics and clinical characteristics of the traumatic brain injury patients

Group	Age	Gender	Time since injury (months)	Cause of Injury	PTA Duration (days)	Lowest GCS	LOC	MRI	Medications
NSM TBI	41	Male	84	Blast	Unknown	3	Yes	Tiny cortical gliotic scar in the right frontal lobe underlying the site of a burr hole relating to previous pressure bolt.	Nil
NSM TBI	35	Male	58	Blast	14	3	Yes	Indented skull vault overlying left frontal and temporal loves. Mature gliotic damage affecting the frontal and temporal cortex.	Nil
ISM TBI	31	Male	52	Blast	Unknown	Unknown	No	Mild generalised volume loss (subjective)	Nil
NSM TBI	32	Male	82	Blast	Unknown	3	Yes	Nil	Pregabalin 300mg BD, Fluoxetine 40mg, Docusate, Amitriptyline 50mg, Fentanyl 50mg, Sevredol PRN, Zomorph 30mg BD, Testosterone & GH
NSM TBI	38	Male	10	Fall	2	4	Yes	Left frontal and left occipital microbleeds	Vitamin D supp. OD
NSM TBI	42	Male	152	RTA	0	15	No	Nil	GH 0.2mg OD, Modafinil 300mg OD, citalopram 20mg OD, Omeprazol 40mg Nebido 1g, Viagra PRN
NSM TBI	37	Male	12	RTA	4	Unknown	Yes	Left inferior frontal and opercular contusion	Omeprazol 40mg OD, Gabapentin 900mg OD, Vitamin D supp. OD
ISM TBI	34	Male	6	Fall	1	Unknown	Yes	Nil	Nil
ISM TBI	59	Male	3	RTA	7	8	Yes	Microbleeds in parafalcine distribution	Nil
ISM TBI	39	Male	7	RTA	0	14	No	Microbleeds in parafalcine distribution, medial temporal lobes and right thalamus	Nil
NSM TBI	48	Female	3	Fall	2	Unknown	Yes	Mature gliotic damage in right temporal pole and inferior temporal gyri. Right frontal gliotic damage.	Ibuprofen
NSM TBI	44	Male	20	RTA	6	12	Yes	Contusions overlying both orbits. Right parietal and left perisylvian cortex microbleeds	Hydrocellulose 10mg, Lansoprazole 30mg
NSM TBI	30	Male	67	Assault	90	Unknown	Yes	Left temporal contusion, gliosis superior vermis	Nil
NSM TBI	23	Female	11	Fall	2	Unknown	Yes	Frontal and temporal pole gliosis	COCP OD
ISM TBI	59	Male	15	RTA	7	3	Yes	Left and right frontal contusions left temporal contusions	Simvastatin 40mg OD, Omeprazole 20mg OD
NSM TBI	61	Male	10.19	RTA	2	Unknown	Yes	Sub-frontal and left frontal pole contusions	Nil
ISM TBI	26	Male	17	RTA	3	14	Yes	Bifrontal and right temporal contusions	Nil
ISM TBI	53	Male	13	Fall	Unknown	8		Bifrontal and bitemporal pole contusions	Lamotrigine 50mg BD
NSM TBI	53	Male	19	Fall	7	10	Yes	Left temporal contusion	Vitamin D supp. OD
NSM TBI	38	Male	41	Assault	3	3	Yes	Left frontal and temporal contusions; left temporal volume loss	Nil

Supplementary Table 1. Demographics and clinical characteristics of the traumatic brain injury patients

ISM TBI	58	Male	6	RTA	7	7	Yes	Bifrontal and right temporal pole contusions	Nil
NSM TBI	40	Male	134	RTA	42	3	Yes	Bifrontal contusions	Nil
NSM TBI	42	Female	48	RTA	3	Unknown	Unknown	Left frontal contusion and diffuse microbleeds	Nil
ISM TBI	40	Female	50	Sports injury	3	Unknown	Yes	Superficial siderosis and right frontal contusion	Nil
ISM TBI	31	Male	42	Sports injury	1	Unknown	Yes	Possible temporal lobe contusion	Nil
NSM TBI	25	Male	15	RTA	14	3	Yes	Microbleeds in parafalcine distribution	Nil
ISM TBI	44	Female	436	RTA	Unknown	Unknown	Unknown	Left temporal and sub-frontal contusions.	Nil
ISM TBI	44	Male	353	RTA	42	3	Yes	Marked volume loss of body and splenium of corpus callosum	Nil
ISM TBI	61	Female	426	RTA	120	5	Yes	Mature gliotic frontal damage. Bilateral frontal microbleeds	Citalopram 10mg OD
ISM TBI	40	Female	370	RTA	Unknown	Unknown	Yes	Bifrontal contusions. Mature gliotic damage in right parietal cortex. Extensive damage extending left temporal pole and posterior frontal lobe.	Carbamazepine 100mg, propanalol 40mg, contraceptive implant
ISM TBI	65	Male	372	Fall	14	Unknown	Yes	Mature cortical infarcts in right medial occipital lobe. Mature damage in left cerebellar	Amlodipine 5mg, Simvastatin 40mg, Ramipril 2.5mg
ISM TBI	54	Male	412	RTA	10	Unknown	Yes	Right frontal, temporal, occipital and parietal contusions. Widespread microbleeds	Tegretol 200mg BD, Cocodamol PRN, Amytriptyline 100mg, Naproxen PRN
ISM TBI	56	Female	415	RTA	80	3	Yes	Mature gliotic damage in the right frontal lobe. Marked loss of volume in the corpus callosum	Statins, Ventolin, Seretide (dosages unknown)
NSM TBI	43	Male	300	RTA	Unknown	3	Yes	Frontal contusions, left temporal pole contusions	Pregabalin 75mg BD, Ventolin, Cetirizine, Omeprazole, Lamotrigine 50mg BD, Paracetamol PRN, Ibuprofen PRN, Codydramol 30:500 PRN
NSM TBI	46	Female	376	Fall	28	3	Yes	Left superior frontal and left middle frontal gyrus contusions. Small amount of cortical damage in right inferior frontal gyrus. Cerebellar atrophy.	Penicillin (dosage unknown)

Supplementary Table 1. Demographics and clinical characteristics of the traumatic brain injury patients

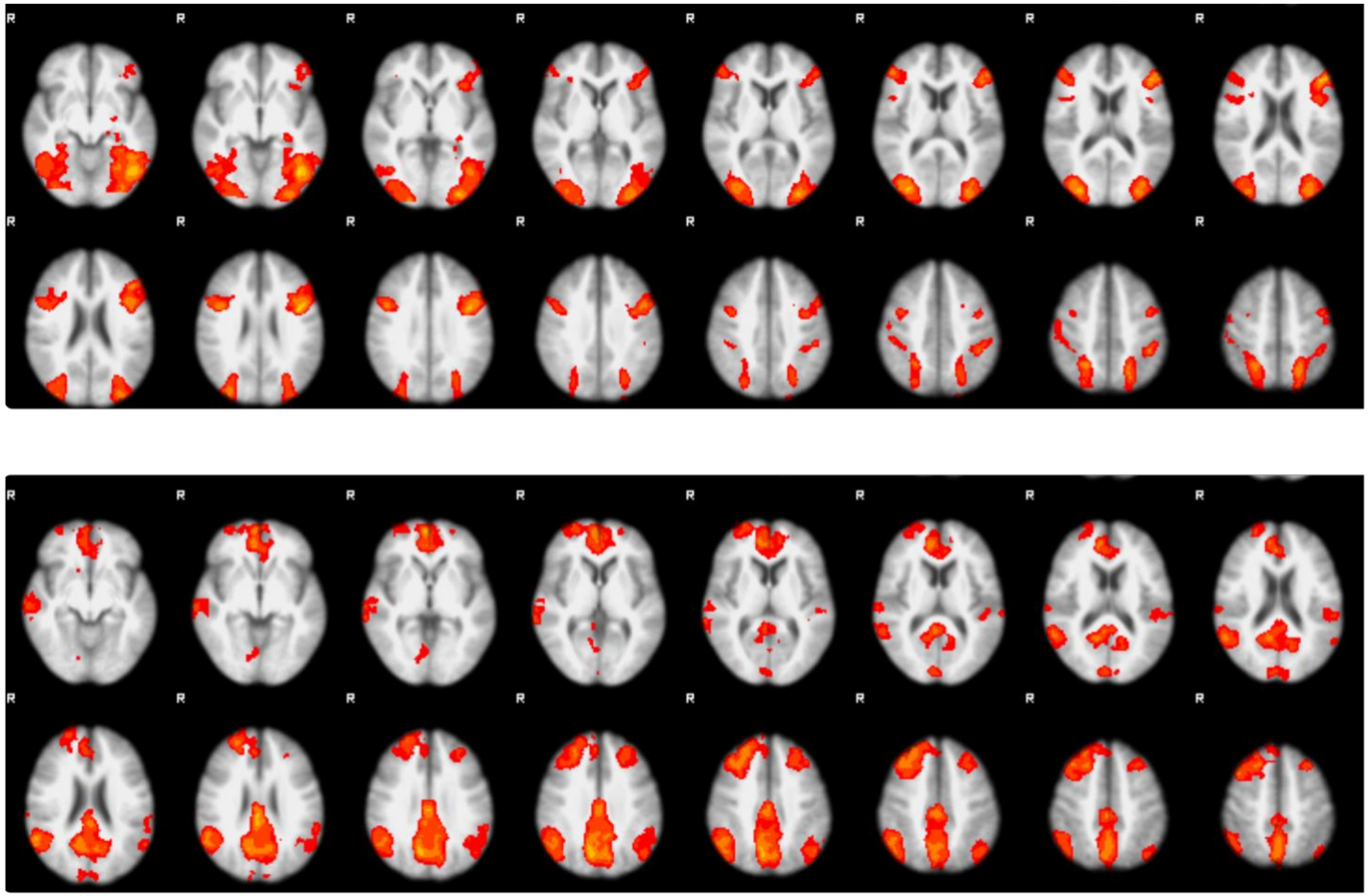

Supplementary Figure 1. Alterations in BOLD activity associated with performance on the memory encoding task. All spatial results shown in standard space overlaid on MNI template with a Z-statistic threshold of 2.3. **Top panel:** All TBI patient. Voxels showing increased activation during successful encoding (remembered minus forgotten contrast) and **Bottom panel:** decreased activation.